Available online at www.sciencedirect.com
ScienceDirect
Carbohydrate Research 343 (2008) 221–229
Carbohydrate RESEARCH

WAXS and ^{13}C NMR study of *Gluconoacetobacter xylinus* cellulose in composites with tamarind xyloglucan

Tracey J. Bootten,[a,†] Philip J. Harris,[a,*] Laurence D. Melton[b] and Roger H. Newman[c,‡]

[a]*School of Biological Sciences, The University of Auckland, Private Bag 92019, Auckland, New Zealand*
[b]*Food Science Programme, The University of Auckland, Private Bag 92019, Auckland, New Zealand*
[c]*Industrial Research Limited, PO Box 31-310, Lower Hutt, New Zealand*

Received 21 December 2006; received in revised form 2 November 2007; accepted 7 November 2007
Available online 17 November 2007

Abstract—- Model composites, produced using cellulose from stationary cultures of the bacterium *Gluconoacetobacter xylinus* and tamarind xyloglucan, were examined by wide-angle X-ray scattering (WAXS) and CP/MAS solid-state ^{13}C NMR spectroscopy. The dominant crystallite allomorph of cellulose produced in culture media with or without xyloglucan was cellulose I_α (triclinic). The presence of xyloglucan in the culture medium reduced the cross-section dimensions of the cellulose crystallites, but did not affect the crystallite allomorph. However, when the composites were refluxed in buffer, the proportion of cellulose I_β allomorph increased relative to that of cellulose I_α. In contrast, cellulose I_α remained the dominant form when cellulose, produced in the absence of xyloglucan, was then heated in the buffer. Hence the presence of xyloglucan has a profound effect on the formation of the cellulose crystallites by *G. xylinus*.

Keywords: Plant cell walls; Xyloglucan; Cellulose; *Gluconoacetobacter xylinus*; Solid-state ^{13}C NMR; WAXS (wide-angle X-ray scattering)

1. Introduction

The primary cell walls of most angiosperms (flowering plants), including the eudicotyledons, non-commelinid monocotyledons and palms (Arecales), consist of cellulose microfibrils set in a matrix composed principally of pectic polysaccharides and xyloglucans.[1] These polysaccharides are thought to form two coextensive networks: one composed of cellulose microfibrils and xyloglucans, and the other of pectic polysaccharides; a third network of the glycoprotein extensin is sometimes also present.[2] Because of the complexity of these cell walls, model composite systems have been used to investigate the interactions among the different constituents. In particular, composites of bacterial cellulose and xyloglucan, produced by culturing the bacterium *Gluconoacetobacter xylinus* in media containing tamarind xyloglucan, have been widely used.[3–8] Similarities were found between the micro-morphological features of these composites and those of primary cell walls when they were viewed by transmission electron microscopy after preparation by fast-freeze, deep-etch and rotary shadowing.[5,8]

In the present study, we investigated the possible effects of the presence of xyloglucan in the culture medium on the structure of the cellulose. To do this, we used composites of *G. xylinus* cellulose and a commercial preparation of tamarind xyloglucan. Studies using transmission electron microscopy have previously shown that *G. xylinus* cellulose forms microfibrils 3–4 nm wide, which aggregate to form bundles 6–12 nm wide, which loosely associate to form ribbons

* Corresponding author. Tel.: +64 9 3737599x88366; fax: +64 9 373 7416; e-mail: p.harris@auckland.ac.nz
† Present address: Industrial Research Limited, PO Box 31-310, Lower Hutt, New Zealand.
‡ Present address: Scion, Private Bag 3020, Rotorua, New Zealand.

0008-6215/$ - see front matter © 2007 Elsevier Ltd. All rights reserved.
doi:10.1016/j.carres.2007.11.008

20–60 nm wide.[9] We used wide-angle X-ray scattering (WAXS) diffractograms and solid-state ^{13}C NMR spectroscopy to examine the dimensions and allomorphs of the cellulose crystallites.

2. Results

2.1. Wide-angle X-ray scattering (WAXS) diffractograms

Crystallographic planes are labelled according to the cellulose I_α structure as described by Sugiyama et al.[10] (see Fig. 1). In diffractograms for the two cellulose-only preparations, peaks from the three main crystallographic planes 1 1 0, 0 1 0 and 1 0 0 could be clearly distinguished (Fig. 2). As the cellulose is a mixture of cellulose I_α and I_β, the peaks are actually pairs of unresolved peaks, one component for each crystalline form. This broadens the observed line shapes and therefore results in a small underestimation of the crystallite dimensions.[11] The diffractograms also showed a relatively narrow peak, centred on 31.2°, from the boron nitride added as the internal standard.

Both loosely and firmly packed samples were examined to test for changes in the preferential alignment of the cellulose crystallites. The alignment of crystallites that are rectangular in cross-section was expected to respond to compaction, with the larger dimension showing preferential alignment parallel to the solid surface as in Figure 3. Obviously there can be no such preferential alignment for crystallites with square cross-sections. The peak assigned to the 0 1 0 plane in diffractograms of the firmly packed samples of both cellulose-only preparations was suppressed (Fig. 2) compared with the same peak in loosely packed samples of the same preparations, as expected for a preferential alignment of the crystallites. This preferential alignment was consistent with a cellulose crystallite cross-section in which the dimension perpendicular to the 0 1 0 planes was greater than that perpendicular to the 1 0 0 planes, as indicated by peak widths (Table 1). The suppression of the 0 1 0 peak in diffractograms of the firmly packed samples, compared with the loosely packed samples of the same preparation, was less evident for the composite preparations, indicating a cross-section that was more square than rectangular.

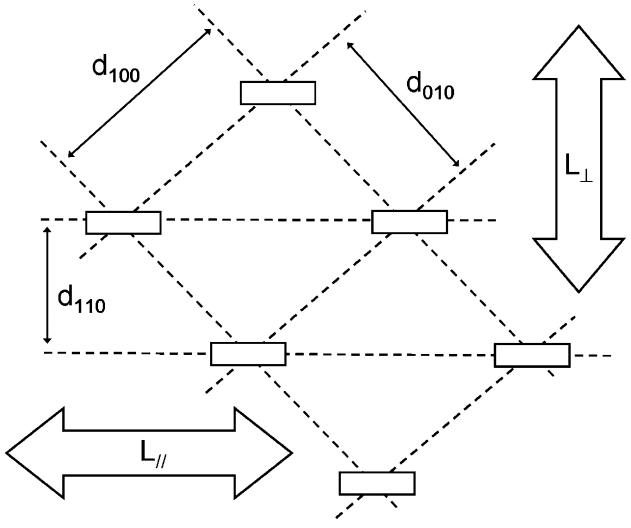

Figure 1. Cross-section through a hypothetical cellulose crystallite containing six cellulose chains, each represented by a rectangle. Broken lines show the lattice planes and block arrows indicate directions for measurement of cross-sectional dimensions.

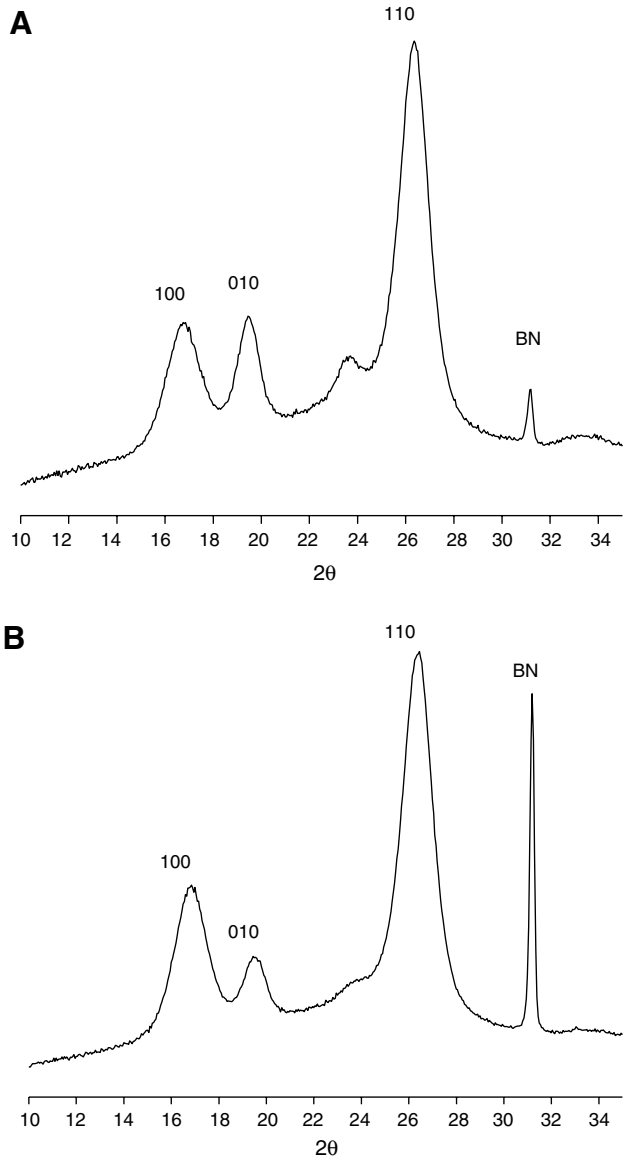

Figure 2. WAXS diffractograms of the heated cellulose-only preparation. A peak from the internal standard of boron nitride (BN) is centred at 31.2°. (A) A loosely packed sample and (B) a firmly packed sample. The planes are labelled according to cellulose I_α as described by Sugiyama et al.[10]

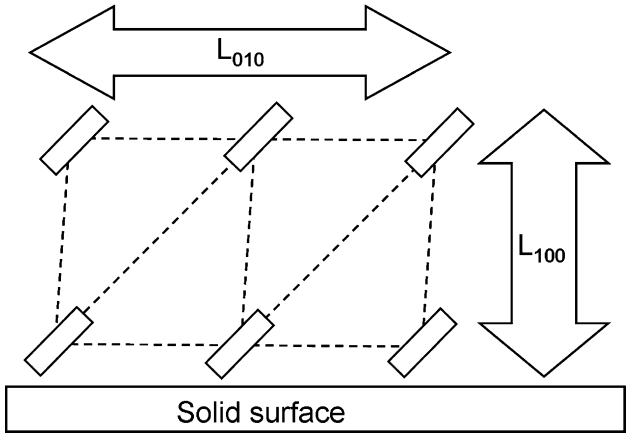

Figure 3. The hypothetical crystallite shown in Figure 1 resting on a solid surface. Block arrows indicate relevant directions for measurement of cross-sectional dimensions.

Diffractograms obtained from both loosely and firmly packed unheated and heated cellulose-only preparations had Bragg angles that corresponded to lattice spacings of $d = 0.613$ nm, 0.529 nm and 0.392 nm for the three main crystallite planes, 100, 010 and 110, respectively. The lattice spacings for the cellulose crystallites in the unheated composite were no different from those in the two cellulose-only preparations. However, in the heated composite, the lattice spacing for the 100 plane was slightly less (0.592 nm) and for the 110 plane slightly more (0.396 nm) than those planes in the cellulose only and the unheated composite preparations. Differences in lattice spacings were considered relevant because they are associated with differences in the cross-sectional dimensions of cellulose crystallites.[12]

Diffractograms of the unheated composite preparation (Fig. 4) showed that the 110 peak was considerably broader than in diffractograms of both the heated (Fig. 2) and unheated (diffractogram not shown) cellulose-only preparations. The thicknesses of the cellulose crystallites calculated using Eq. 1 were $L_{\perp} = 5.9$ and 6.0 nm for the heated and unheated cellulose-only preparations, respectively, and 4.7 nm for the unheated composite preparation (Table 1). Here $L_{\perp} = L(110)$, that is, the cross-sectional dimension measured perpendicular to the sheets of cellulose chains (Fig. 1). This indicates that the thickness of the cellulose crystallites was significantly less when xyloglucan was included in the medium.

Heating the composite preparation broadened the 110 peak in the WAXS diffractogram (diffractogram not shown), indicating a further decrease in cellulose crystallite thickness (Table 1) or an increase in packing defects.

Relative peak widths provided an indication of the cross-sectional shape of the cellulose crystallites. For the unheated and heated cellulose-only preparations, the width of the 010 peak was less than that of the 100 peak. The corresponding dimensions (Table 1) indi-

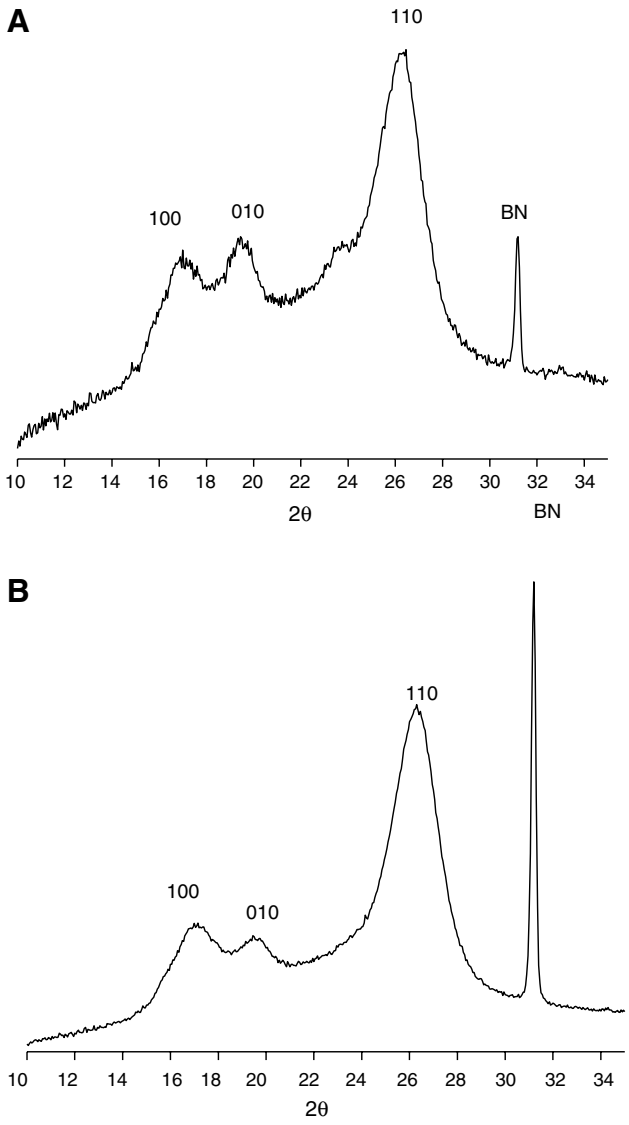

Figure 4. WAXS diffractograms of the unheated cellulose–xyloglucan composite. A peak from the internal standard of boron nitride (BN) is centred at 31.2°. (A) A loosely packed sample and (B) a firmly packed sample. The planes are labelled according to cellulose I_{α} as described by Sugiyama et al.[10]

Table 1. Cellulose crystallite thicknesses[a] (L measured perpendicular to the specified planes = $L_{\perp}$) in the preparations obtained from WAXS diffractograms (LP, loosely packed sample; FP, firmly packed sample)

Preparation		L_{100} (nm)	L_{010} (nm)	L_{110} (nm)
Unheated cellulose-only	LP	5.5	7.8	6.0
	FP	5.8	7.2	5.9
Heated cellulose-only	LP	5.2	6.7	5.9
	FP	5.2	6.7	5.9
Unheated composite	LP	—[b]	—[b]	4.7
	FP	—[b]	—[b]	4.7
Heated composite	LP	—[b]	—[b]	3.6
	FP	—[b]	—[b]	3.6

[a] Calculated using Eq. 1 with $K = 0.9$, which is appropriate for crystallites with square cross-sections.

[b] Peaks too poorly resolved to measure the widths and determine L.

cated that the cross-sections of the cellulose crystallites were relatively extended in the direction perpendicular to the 010 planes. The peaks assigned to the 100 and 010 crystal planes in the diffractograms from the composite preparations were too poorly resolved to measure the peak widths and thus determine cross-sectional dimensions. In these diffractograms, the xyloglucan in the composite was expected to contribute to a broad background under the sharper cellulose peaks.

2.2. Solid-state CP/MAS NMR spectroscopy

The CP/MAS NMR spectra obtained from the unheated and heated cellulose-only preparations showed peaks that could all be assigned to the Glc residues of cellulose (Fig. 5A and B). The spectra were similar to those obtained by Yamamoto and Horii[6] for cellulose from the same species. The CP/MAS NMR spectra of the unheated and heated composite preparations (Fig. 6A and B) were also dominated by sharp signals that can be assigned to cellulose. Further, the signals at 99–100 ppm can be assigned to xylose (C-1) of xyloglucan[5] and at 80 ppm to glucose (C-4) of xyloglucan,[5] indicating that xyloglucan was associated with the cellulose in both composite preparations. Other signals from xyloglucan were presumed to overlap with the dominant signal strengths from the cellulose, both in the C-1 and in the C-4 regions of the CP/MAS spectrum.

In common with cellulose from other sources, including angiosperm cell walls, the NMR signals from cellulose overlapped in the C-1 region of the CP/MAS spectrum, whereas there were distinct signals from C-4 for the cellulose in the crystallite interior (89 ppm) and on the crystallite surface (85 ppm) (Fig. 7).[13,14] The C-6 region showed a similar splitting of the signals assigned to the cellulose in the crystallite interior (66 ppm) and on the crystallite surface (63 ppm). The

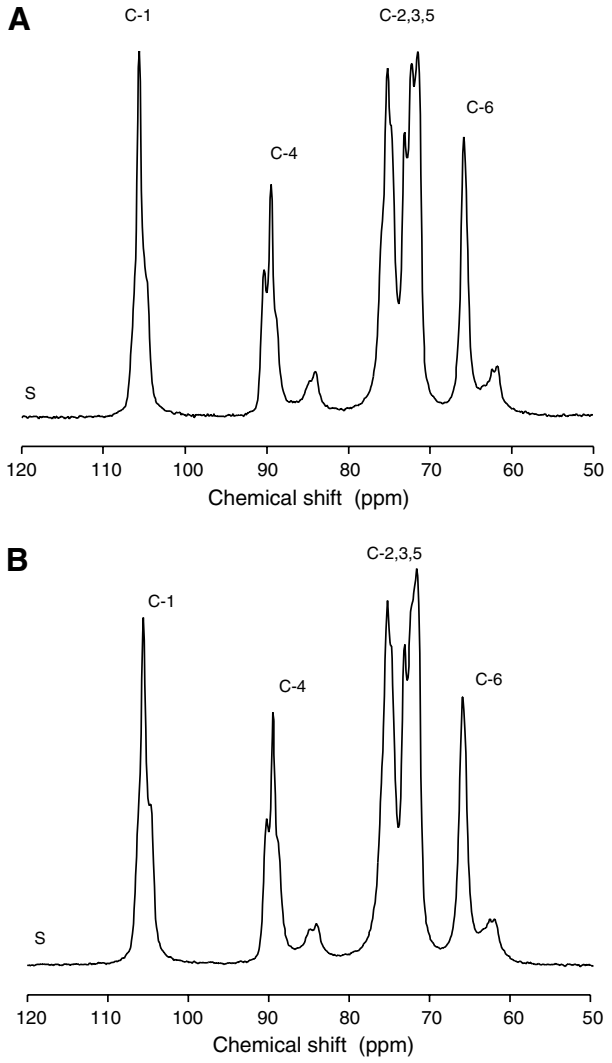

Figure 5. CP/MAS NMR spectra of cellulose-only preparations: (A) the unheated preparation and (B) the heated preparation. Carbon numbers refer to those assigned to the glucosyl residues of cellulose.

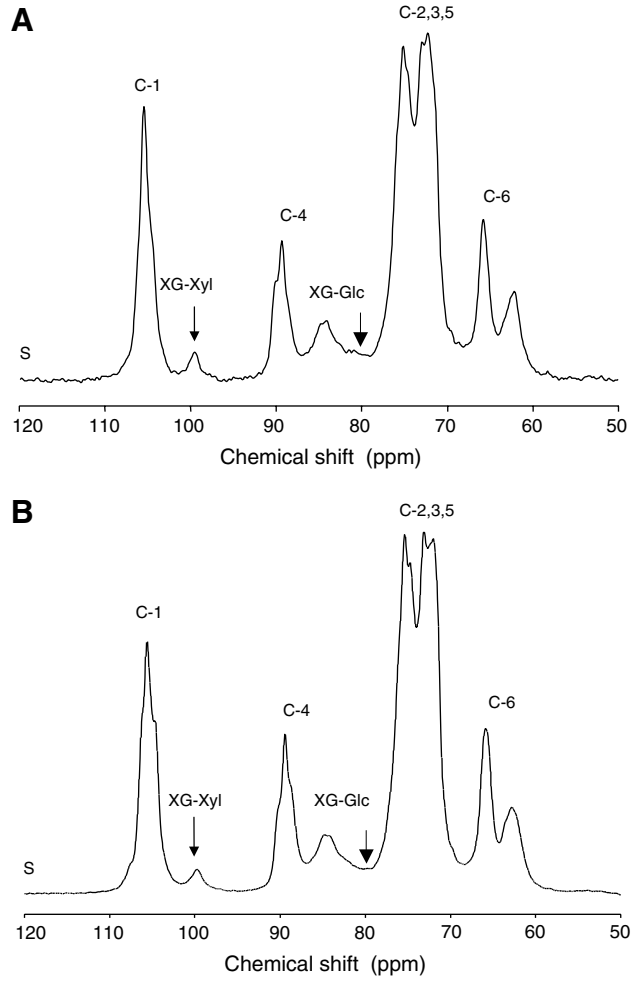

Figure 6. CP/MAS NMR spectra of cellulose–xyloglucan composite preparations: (A) the unheated preparation and (B) the heated preparation. Carbon numbers refer to the glucosyl residues of cellulose. Arrows indicate assignments to tamarind XG.

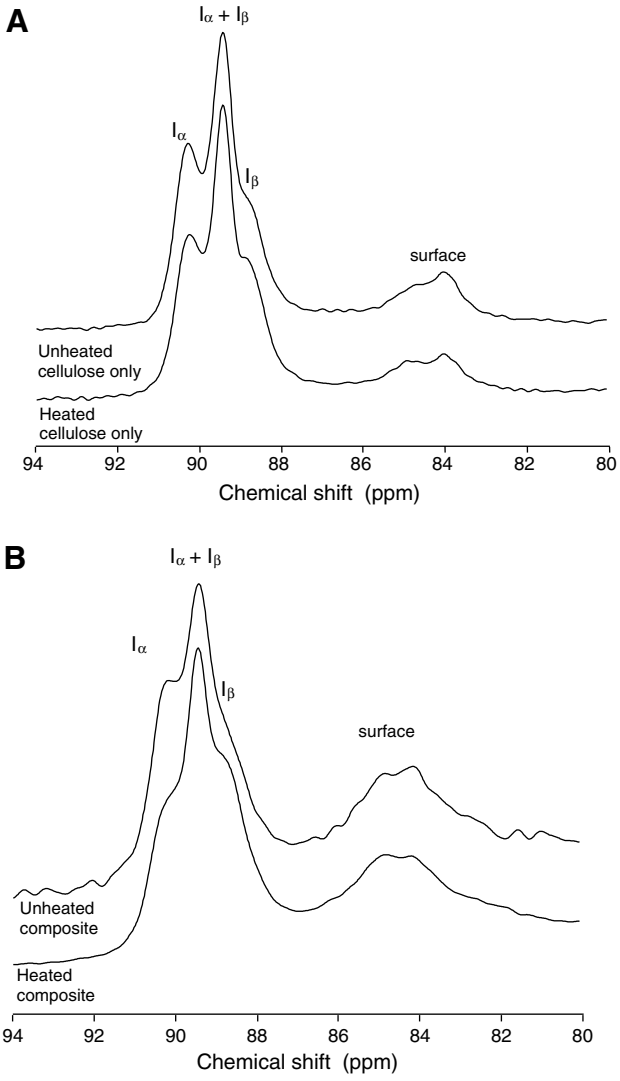

Figure 7. Expanded portions of the C-4 regions of the CP/MAS spectra: (A) the unheated and heated cellulose-only preparations and (B) the unheated and heated composite preparations. Signals are assigned to crystallite-interior cellulose in two allomorphs.

areas under the 89 and the 85 ppm signals were 81% and 19%, respectively, indicating that the cellulose molecules in both cellulose-only preparations were mostly in the interior of the crystallites.

The areas under the crystallite interior and crystallite surface peaks, 89 and 85 ppm, respectively, were used to calculate the dimension along planes parallel to the hydrogen-bonded sheets of the cellulose crystallite ($L_{\|}$).[15] The dimension $L_{\|}$ is defined in Figure 1. Using Eq. 2, both the unheated and heated cellulose-only preparations had an average $L_{\|}$ dimension of 8.6 nm (Table 2), corresponding to an average of 11 cellulose chains in the plane of the cellulose sheet. NMR signals from the two cellulose I allomorphs, cellulose I_α (triclinic) and cellulose I_β (monoclinic), were also separated in the C-4 region of the NMR spectrum (Fig. 7A), with signals

Table 2. The proportion of interior and surface cellulose molecules and dimensions of the cellulose crystallites in the preparations as the mean width of sheets of chains ($L_{\|}$) determined by ^{13}C NMR spectroscopy

Preparation	% Interior	% Surface	$L_{\|}$ (nm)
Unheated cellulose-only	81	19	8.6
Heated cellulose-only	81	19	8.6
Unheated composite	70	30	5.5
Heated composite	72	28	5.9

at 90.2 ppm for cellulose I_α and signals at 88.5 ppm for cellulose I_β and signal strength at 89.4 ppm assigned to both celluloses I_α and I_β. Signals in the C-4 region of the CP/MAS spectra obtained from the unheated and heated cellulose-only preparations (Fig. 7A), and assigned to the interior crystallites, showed that the cellulose consisted of more cellulose I_α than cellulose I_β. In the heated cellulose-only preparation, the proportion of cellulose I_β was slightly higher than in the unheated cellulose-only preparation, but cellulose I_α remained the dominant crystal form. Cellulose I_α was also the dominant crystal form in the unheated composite preparation (Fig. 7B). However, in the heated composite preparation (Fig. 7B), there was more cellulose I_β than cellulose I_α.

2.3. Proton spin-relaxation editing (PSRE) of the cellulose/xyloglucan composites

PSRE exploited the differences in proton spin–spin relaxation, with time constant T_2(H), between the normal CP/MAS spectrum and a spectrum obtained with proton–spin relaxation experiments (Fig. 8), to separate signals into two subspectra (Fig. 9). Subspectrum A had signals with short values of T_2(H) assigned to the rigid cellulose, whereas subspectrum B had signals with longer values of T_2(H) assigned to polymers more mobile than cellulose. The two cellulose-only preparations showed no differential relaxation of the NMR signals in the proton relaxation experiments, indicating that all of the cellulose molecules were of similar rigidity.

In PSRE experiments on the unheated (Fig. 9A) and heated composite preparations (Fig. 9B), the separation of subspectra was successful if the 89 ppm signal, unique to the rigid interior of the cellulose crystallites, was eliminated from subspectrum B, and the signal strength at 80 ppm, assigned to relatively mobile xyloglucan, was eliminated from subspectrum A.

The inclusion of xyloglucan in the culture medium altered the proportion of crystallite interior and surface cellulose molecules in the composite preparations as determined by the area under the C-4 signals assigned to the cellulose crystallite interior and crystallite surface in subspectrum A (Table 2). The dimensions parallel to the plane of the sheet ($L_{\|}$) of the cellulose crystallites in

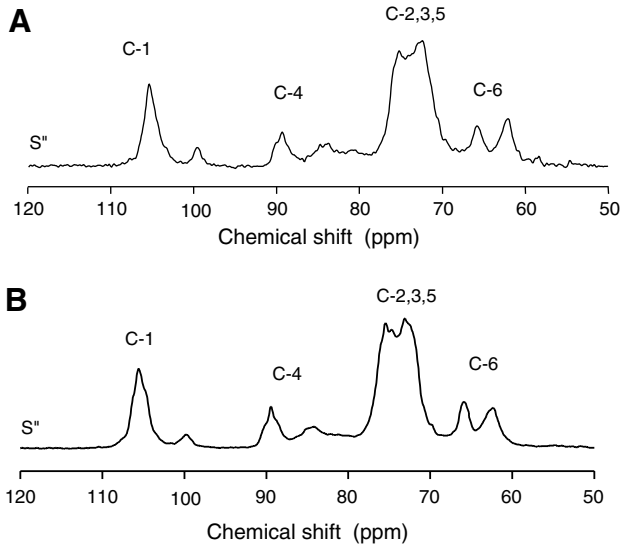

Figure 8. Solid-state CP/MAS ^{13}C NMR spectra of composite preparations obtained with 15 μs of proton spin–spin relaxation. (A) The unheated composite preparation and (B) the heated composite preparation. Carbon numbers refer to the glucosyl residues of cellulose.

the composite preparations were determined from the areas under the C-4 signals, assigned to the cellulose crystallite interior and crystallite surface (Table 2). For the unheated and heated composite preparations, the value of X (see Eq. 2) was considerably reduced compared to the cellulose-only preparations, indicating that the cross-sectional dimensions $L_{\|}$ of the crystallites were considerably smaller (Table 2), corresponding to crystallites with an average of seven to eight cellulose chains in planes parallel to the crystallite sheets. There was no significant changes in $L_{\|}$ associated with heating the cellulose-only preparation or the composite.

3. Discussion

Unlike previous studies, we showed that it is possible to include unmodified tamarind xyloglucan in the *G. xylinus* culture medium without altering the proportion of cellulose I_β. In experiments using similar conditions, Whitney et al.[8] used two different tamarind xyloglucan preparations (molecular weights 880 and 230 kDa). They examined the effects of the higher molecular weight preparation using both static and agitated culture conditions, but only agitated culture conditions were used with the lower molecular weight preparation. Under agitated conditions, both xyloglucan preparations yielded cellulose with a 40:60 ratio of I_α:I_β, suggesting that molecular weight is not an important factor in altering the proportions. Under static conditions, the higher molecular weight preparation yielded cellulose with a 50:50 I_α:I_β ratio, indicating that agitation of the medium increased the proportion of cellulose I_β. Much lower

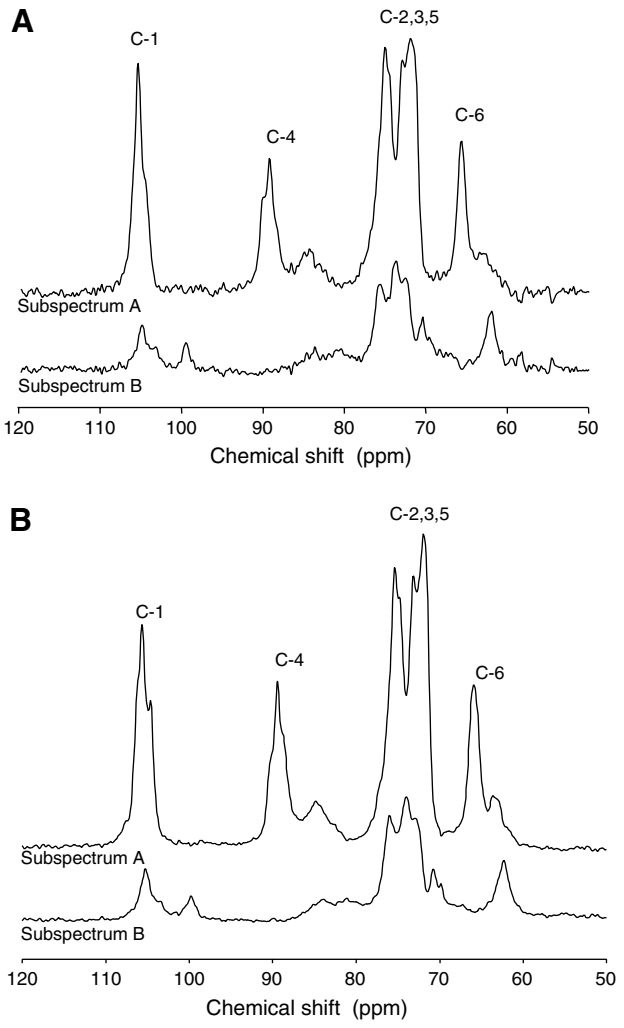

Figure 9. PSRE subspectra separated from the normal CP/MAS spectrum of the unheated and heated composite preparations, by exploiting differences in proton spin–spin relaxation. (A) The unheated composite preparation and (B) the heated composite preparation. Subspectrum A and subspectrum B display signals assigned primarily to cellulose and the XG, respectively. Carbon numbers refer to glucosyl residues of cellulose.

proportions of cellulose I_β were obtained under static conditions without adding xyloglucan (70:30 I_α:I_β). Thus, from comparisons with the results of Whitney et al.,[8] it is not clear why, without heating, the particular xyloglucan preparation we used caused no increase in the proportion of cellulose I_β. In their study, Whitney et al.[8] examined composites formed from a range of xyloglucan preparations and found an increase in the proportion of cellulose I_β to at least half of the two allomorphs for all except a composite obtained using a tamarind xyloglucan preparation, which had 60% of the galactose removed by a β-galactosidase. It would be interesting to know if the proportion of cellulose I_β in this composite could be increased by heating.

Some of the researchers who reported an increased proportion of cellulose I_β when xyloglucan was included

in the culture medium heated the composite and the control cellulose in dilute alkali before examining it by solid-state ^{13}C NMR spectroscopy. For example, Hackney et al.[3] and Yamamoto and Horii[6] boiled them in 1% aqueous sodium hydroxide for 6 and 8 h, respectively. From their results, it cannot be established whether the increased proportions of cellulose I_β occurred before or after heating.

However, the change from cellulose I_α to cellulose I_β as the dominant allomorph was not a consequence of heating alone. In our study, the CP/MAS NMR spectrum of the heated cellulose-only preparation showed only a slightly greater proportion of cellulose I_β compared with the unheated cellulose-only preparation, with cellulose I_α remaining the dominant allomorph. For near-complete conversion of cellulose I_α to cellulose I_β, Debzi et al.[16] found that it was necessary to heat bacterial cellulose to a higher temperature (260 °C) in saturated steam. Our study therefore showed that including the tamarind xyloglucan preparation in the culture medium lowered the critical temperature for conversion of cellulose I_α to cellulose I_β.

To obtain the cellulose crystallite widths ($L_{\|}$) measured across the 1 1 0 plane, that is, across the sheets of chains,[15] we used solid-state ^{13}C NMR spectra. The value of $L_{\|}$ was 5.5 nm for our unheated composite preparation compared with 8.6 nm for our unheated cellulose-only preparation. The smaller cellulose crystallites in the unheated composite preparation may have facilitated the conversion of cellulose I_α to cellulose I_β when the composite was heated. A mechanism for the conversion of cellulose I_α to I_β has been proposed[17] that involved slippage of the cellulose chains past one another, aided by expansion of the cellulose sheets in the stacking direction when the cellulose was heated. It is envisaged that the smaller crystallite size with reduced crystallinity, of the bacterial cellulose produced in medium containing XG, may have aided in this slippage.

The crystallite cross-sectional dimensions provided by WAXS are important for characterising the shapes of the cellulose crystallites. Our results for the cellulose-only preparations indicated a rectangular cross-section with $L_{010} > L_{100}$. The absolute values of the dimensions calculated from Eq. 1 are only an approximation because a value was used for K (0.9) derived for square cross-sections,[18] which is the best estimate available. The WAXS results were consistent with the NMR results in demonstrating smaller crystallite cross-sections for cellulose synthesised in the presence of xyloglucan.

A close association of tamarind xyloglucan with cellulose crystallites at the point of ribbon formation may disrupt the cohesion of the cellulose ribbon. The inclusion of xyloglucan in the medium has been shown to disrupt the normal assembly of the bacterial cellulose ribbon and has been compared with the effect of carboxymethylcellulose (CMC) on the formation of the bacterial cellulose ribbons.[6,19,20] Other non-cellulosic polysaccharides such as heteroxylans[4,20–22] and glucomannans[3,4,21,23] also affected the assembly of the bacterial cellulose ribbons at the same stage as CMC. The disruption of the assembly of the normal cellulose ribbons by non-cellulosic polysaccharides appears to be correlated with the ability of the non-cellulosic polysaccharide to hydrogen bond to cellulose in vitro, providing circumstantial evidence for the hydrogen-bonding of non-cellulosic polysaccharides to crystallite surfaces.

In the present study, the disruption of the bacterial cellulose ribbons by the inclusion of xyloglucan in the bacterial culture medium was also detected by the changes to the WAXS diffractograms when the composite preparations were firmly packed. The unheated cellulose-only preparation showed a change in the preferential alignment of the cellulose crystallites when pressed into a pellet. This effect is consistent with the preferred alignment of the crystallites with the 1 0 0 plane parallel to the surface of the disc. This alignment was also observed by Tokoh et al.[23] by changing the irradiation angle in WAXS experiments of cellulose from *G. xylinus*. Our unheated composite preparation likewise showed a change in the preferential alignment of the cellulose crystallites when pressed into a pellet. The changes in the WAXS patterns probably reflect the extent of alignment of the fibres caused by the compression, rather than a change in shape of the crystallites themselves. However, the preferred alignment might also have reflected the shape of the ribbon within which the crystallites were embedded.

Tokoh et al.[20,22] proposed a mechanism for the disruption of the assembly of the bacterial cellulose ribbon by heteroxylans. In this mechanism, heteroxylans interacted with the cellulose molecules on the surface of the crystallites inhibiting complete crystallisation of the microfibril. This would result in crystallites with a reduced cross-sectional area.[22] A similar mechanism may also apply to the cellulose/xyloglucan composites reported in the present study.

4. Experimental

4.1. Preparations of cellulose and cellulose–xyloglucan composites

G. xylinus ssp. *xylinus* (ATCC 53524) (formerly *Acetobacter xylinum*) was incubated at 28 °C for four days under stationary conditions[6] in Hestrin–Schramm medium[24] (pH 6) containing 2% (w/v) glucose only or 2% (w/v) glucose and 0.5% (w/v) tamarind xyloglucan (average MW 212,000 Da determined by multi-angle light scattering (MALS); Megazyme International Ireland Ltd, County Wicklow, Ireland). The pellicles were

harvested, suspended in water (250 mL; 4 °C) and homogenised using a blender (Polytron Model PT10-35, Kinematica, Luzern, Switzerland) on full power for 20 s. The homogenate was poured onto a 50-μm nylon mesh and washed with water (2 L), giving unheated cellulose-only and unheated cellulose–xyloglucan composite preparations.

Heated cellulose-only and cellulose–xyloglucan composite preparations were prepared as above by refluxing (100 °C; 72 h)[25] in sodium acetate buffer (25 mM, pH 5.8).[26]

Aliquots were removed from the four preparations and freeze-dried for WAXS experiments. For solid-state ^{13}C NMR experiments, the remainder of the preparations was partially dried to approximately 50% (w/w) water content by using a freeze drier.

4.2. Wide-angle X-ray scattering (WAXS) diffractograms

Freeze-dried preparations were mixed with the internal standard boron nitride (1% w/w) and examined with a diffractometer (Model D8, Bruker, Madison, Wisconsin, USA) using monochromated Co K_α radiation ($\lambda = 0.179026$ nm) and a parallel-beam geometry. A value of $2\theta = 31.20°$ was determined for the boron nitride powder by calibration against standard silicon (NIST SRM640b) using a Huber 620 Guinier camera. Diffractograms were obtained using a loosely packed and then a firmly packed pellet, to test for changes in the orientations of the cellulose crystallites. Baselines were drawn from 14° to 32° in the same way for all diffractograms.

Cross-sectional dimensions of cellulose crystallites, measured perpendicular to 1 1 0, 0 1 0 and 1 0 0 planes, were estimated from the widths (B) of respective peaks in WAXS diffractograms using the Scherrer equation[27]:

$$L = K\lambda/(B\cos\theta) \quad (1)$$

Here $\lambda = 0.179026$ nm is the wavelength of the radiation, B is the full width (in radians) of the peak (measured at half maximum height), and 2θ is the angle between the incident and diffracted rays. A value of $K = 0.9$ is appropriate for crystallites with a square cross-section.[18] K-values have not been determined for crystallites with rectangular cross-sectional shapes. The subscript attached to $L_\perp$ indicates a value of L measured perpendicular to the 1 1 0 planes, that is, perpendicular to the sheets of cellulose chains (Fig. 1).

4.3. Solid-state ^{13}C NMR spectroscopy

Partially-dried samples were packed in 7-mm diameter, cylindrical silicon nitride rotors, and retained with Vespel end caps. Polydimethylsilane was added to all samples as an internal standard, providing a single sharp signal at −1.96 ppm.[28] The rotor was spun at 4 kHz in a Doty Scientific magic-angle spinning probe for ^{13}C NMR spectroscopy at 50.3 MHz on a Varian Inova-200 spectrometer. Cross-polarisation (CP) NMR experiments were done as described in Bootten et al.[29] Proton spin-relaxation editing (PSRE) of proton spin–spin relaxation (T_2(H)) experiments was performed as described in Bootten et al.,[29] except that the signal strength at 80 ppm assigned to C-4 of glucose in xyloglucan[30,31] was selected as a representative of mobile XG. Proton spin information diffuses across molecular dimensions during the cross-polarisation contact time, so that it is difficult to distinguish values of T_2(H) for monosaccharide residues less than 1 nm apart. It is thus not possible to distinguish T_2(H) values for the XG backbone and sidechains, or for cellulose crystallite-interior and crystallite-surface chains. Details of the suppression factors used to edit the CP/MAS spectra for PSRE and time constants for spin–spin relaxation experiments are shown in Table 3.

Table 3. Suppression factors and resulting linear combinations used to obtain PSRE subspectra from CP/MAS NMR spectra

	Unheated composite preparation	Heated composite preparation
Suppression factors		
f_a	0.21	0.23
f_b	0.48	0.53
Linear combinations		
Subspectrum A	$1.78S - 3.75S''$	$1.77S - 3.33S''$
Subspectrum B	$-0.78S + 3.75S''$	$-0.77S + 3.33S''$

Cross-sectional dimensions of cellulose crystallites, $L_\parallel$ measured parallel to the sheets of cellulose chains, were determined from the areas under the peaks assigned to cellulose in the C-4 region of CP/MAS using the rationale and equation reported by Newman and Davidson.[15] That is, if there are n chains in an averaged cellulose sheet and each cellulose chain is hydrogen bonded to two others except for the two outside chains, which are only attached to one other chain, then X, being the area under the signals assigned to the crystallite interior divided by the total area between 80 and 94 ppm, will be equal to $(n-2)/n$.[15] Thus, X provides an indication of the size of the crystalline domain or the crystallinity.[32] Therefore, $L_\parallel$ can be calculated using the equation,

$$L_\parallel = 2b/(1 - X) \quad (2)$$

where $b = 0.82$ nm is the width of the addition of a cellulose chain in the crystallite.[10]

Acknowledgements

This work was supported by the Marsden Fund of the Royal Society of New Zealand (Grant No. UOA806).

Dr Martin Ryan is gratefully acknowledged for assisting with the WAXS experiments.

References

1. Harris, P. J. In *Plant Diversity and Evolution: Genotypic and Phenotypic Variation in Higher Plants*; Henry, R. J., Ed.; CAB International Publishing: Wallingford, Oxon, UK, 2005; pp 201–227.
2. Harris, P. J. *New Zealand J. Forest. Sci.* **2006**, *36*, 36–53.
3. Hackney, J. M.; Atalla, R. H.; VanderHart, D. L. *Int. J. Biol. Macromol.* **1994**, *16*, 215–218.
4. Uhlin, K. I.; Atalla, R. H.; Thompson, N. S. *Cellulose* **1995**, *2*, 129–144.
5. Whitney, S. E. C.; Brigham, J. E.; Darke, A. H.; Reid, J. S. G.; Gidley, M. J. *Plant J.* **1995**, *8*, 491–504.
6. Yamamoto, H.; Horii, F. *Cellulose* **1994**, *1*, 57–66.
7. Yamamoto, H.; Horii, F.; Hirai, A. *Cellulose* **1996**, *3*, 229–242.
8. Whitney, S. E. C.; Wilson, E.; Webster, J.; Bacic, A.; Reid, J. S. G.; Gidley, M. J. *Am. J. Bot.* **2006**, *93*, 1402–1414.
9. Haigler, C. H.; Brown, R. M.; Benziman, M. *Science* **1980**, *210*, 903–906.
10. Sugiyama, J.; Vuong, R.; Chanzy, H. *Macromolecules* **1991**, *24*, 4168–4175.
11. Fink, H.-P.; Hofmann, D.; Philipp, B. *Cellulose* **1995**, *2*, 51–70.
12. Ioelovich, M.; Larina, E. *Cell. Chem. Technol.* **1999**, *33*, 3–12.
13. Newman, R. H.; Ha, M.-A.; Melton, L. D. *J. Agric. Food Chem.* **1994**, *42*, 1402–1406.
14. Newman, R. H. *Holzforschung* **1998**, *52*, 157–159.
15. Newman, R. H.; Davidson, T. C. *Bot. Mar.* **2004**, *47*, 490–495.
16. Debzi, E. M.; Chanzy, H.; Sugiyama, J.; Tekely, P.; Excoffier, G. *Macromolecules* **1991**, *24*, 6816–6822.
17. Nishiyama, Y.; Sugiyama, J.; Chanzy, H.; Langan, P. *J. Am. Chem. Soc.* **2003**, *125*, 14300–14306.
18. Murdock, C. C. *Phys. Rev.* **1930**, *35*, 8–23.
19. Haigler, C. H.; White, A. R.; Brown, R. M.; Cooper, K. M. *J. Cell Biol.* **1982**, *94*, 64–69.
20. Tokoh, C.; Takabe, K.; Sugiyama, J.; Fujita, M. *Cellulose* **2002**, *9*, 351–360.
21. Iwata, T.; Indrarti, L.; Azuma, J.-I. *Cellulose* **1998**, *5*, 215–228.
22. Tokoh, C.; Takabe, K.; Sugiyama, J.; Fujita, M. *Cellulose* **2002**, *9*, 65–74.
23. Tokoh, C.; Takabe, K.; Fujita, M.; Saiki, H. *Cellulose* **1998**, *5*, 249–261.
24. Hestrin, S.; Schramm, M. *Biochem. J.* **1954**, *58*, 345–352.
25. Newman, R. H.; Hemmingson, J. A. *Carbohydr. Polym.* **1998**, *36*, 167–172.
26. Vincken, J.-P.; de Keizer, A.; Beldman, G.; Voragen, A. G. J. *Plant Physiol.* **1995**, *108*, 1579–1585.
27. Klug, H. P.; Alexander, L. E. *X-ray Diffraction Procedures for Polycrystalline and Amorphous Materials*, 2nd ed.; John Wiley & Sons: New York, 1974, pp 491–538.
28. Earl, W. L.; VanderHart, D. L. *J. Magn. Reson.* **1982**, *48*, 35–42.
29. Bootten, T. J.; Harris, P. J.; Melton, L. D.; Newman, R. H. *J. Exp. Bot.* **2004**, *55*, 571–583.
30. York, W. S.; Harvey, L. K.; Guillen, R.; Albersheim, P.; Darvill, A. G. *Carbohydr. Res.* **1993**, *248*, 285–301.
31. Braccini, I.; Hervé du Penhoat, C.; Michon, V.; Goldberg, R.; Clochard, M.; Jarvis, M. C.; Huang, Z.-H.; Gage, D. A. *Carbohydr. Res.* **1995**, *276*, 167–181.
32. Newman, R. H. *Solid State Nucl. Magn. Reson.* **1999**, *15*, 21–29.